European Journal of Medical Research

RESEARCH

Open Access

Causal relationship analysis of MRI measurements of major human internal organs and liver disease

Huanyu Wu[1], Danjing Zhou[1], Jinggang Zhu[1] and Jianchun Tu[1*]

Abstract

Background This study aimed to explore the causal association between imaging measurement indicators of major internal organs and liver lesions using a two-sample Mendelian randomization (MR) method.

Methods Data from the UK Biobank and GWAS Catalog platform were used to select single nucleotide polymorphisms (SNPs) associated with MRI or derived measurement results of various organ indicators as genetic instrumental variables. Data from the FinnGen project's R9 version were used to select liver lesion outcomes, such as nonalcoholic fatty liver disease (NAFLD), nonalcoholic cirrhosis, and primary hepatocellular carcinoma (HCC). UVMR analysis were utilized variable-by-variable, and MVMR was used to adjust for confounding on significant variables. Steiger directional test, heterogeneity, pleiotropy, and sensitivity tests were conducted to enhance reliability.

Results Univariate Mendelian randomization analysis (UVMR) indicated that liver volume (LV), liver fat (LF), and subcutaneous adipose tissue measurement (SATM) are risk factors for NAFLD. The multivariable MR (MVMR) results for NAFLD showed that LV and LF remained significant, while SATM did not. For cirrhosis (NAC), UVMR suggested that LV, LF, and SATM are risk factors, but MVMR results showed that only LV and LF remained significant. Additionally, pancreatic volume (PV) was found to be a protective factor, while splenic volume (SV) was a pathogenic factor for NAC. For HCC, both UVMR and MVMR analyses suggested that LF and liver iron (LI) are risk factors, while SATM did not remain significant in the MVMR analysis.

Conclusions LV, LF, and SATM are associated with NAFLD. In the NAC stage, additional pathogenic effects of PV and SV were observed. The related results for LF and LI support the pathogenic effect of liver iron factors in the HCC stage.

Keywords Nonalcoholic fatty liver disease, Cirrhosis, Liver cancer, Mendelian randomization, Genome-wide association analysis, Organs, MRI measurements

Background

Liver lesions encompass a sequence of deteriorative clinical and pathological stages, typically reflecting the progression from simple fatty liver (SFL) to steatohepatitis, liver fibrosis, cirrhosis, and eventually liver cancer. Current estimates suggest that nearly 400 million individuals in China are afflicted with liver disorders [1]. Among these, nonalcoholic fatty liver disease (NAFLD) constitutes about 200 million cases, representing 50% of the total, while alcoholic liver disease accounts for 60 million cases, or 15%. The remainder encompasses various forms of hepatitis and more severe conditions. Fatty liver, the preliminary phase of liver pathology, includes a significant portion of these cases. With rising rates of obesity

*Correspondence:
Jianchun Tu
kstcmtujc@sina.com
[1] Department of Radiology, Kunshan Hospital of Chinese Medicine, Suzhou 215300, China

and diabetes globally, NAFLD has emerged as the predominant form of chronic liver disease worldwide [2]. Characterized primarily by an excessive accumulation of fat in liver cells, NAFLD is not associated with alcohol or other known hepatic insults but is linked to insulin resistance and genetic factors. This condition can progress from SFL to nonalcoholic steatohepatitis and eventually to cirrhosis. Although individuals with SFL typically experience favorable outcomes, those with steatohepatitis may advance to cirrhosis, liver cancer, or liver failure, which can be fatal. Consequently, the detection and management of fatty liver and its associated diseases are garnering increasing attention.

Imaging examinations, notably magnetic resonance imaging (MRI), play a pivotal role in the clinical diagnosis of liver disease and organ measurements. These methods enable physicians to assess liver lesions and organ scales to aid the diagnosis. Recent advancements in MRI technology, particularly the use of fast and ultrafast sequences, have demonstrated significant benefits and potential for diagnosing liver lesions using related internal organ measurements [3], as also various health issues, including obesity, malnutrition, osteoporosis, edema, and metabolic syndrome [4–6]. The measure parameters included body mass index (BMI), visceral fat, total body water, muscle mass, basal metabolic rate, and metabolic age [7–9]. Since its introduction in clinical settings, MRI has become widely adopted due to its superior soft tissue resolution and capability for multiparametric imaging. As technology progresses, liver MRI not only provides anatomical visuals, but also delivers functional insights into pathophysiology and metabolism. Moreover, advancements in technology have enabled the acquisition of large-scale whole-body MRI data, offering more precise measurements of body composition compared to conventional metrics, such as BMI [10, 11].

This study employs a two-sample MR approach to analyze genome-wide association study (GWAS) data and examine the causal links between imaging measures of key visceral organs and liver lesions. From a large number of relevant research reports, we have sorted out the following indicators that are extremely relevant to metabolic and cycle function, which including the composition and volume of liver, spleen, lungs, and pancreas. By using structural MRI or related body composition measurements as genetic instrumental variables, Mendelian randomization (MR) studies were conducted to explore associations with disease outcomes. MR studies, leveraging the random distribution of genetic variants, circumvents these issues and MR studies obeyed assumptions including: (i) relevance: the genetic variant is associated with the exposure of interest. (ii) Independence: the genetic variant is independent of the outcome, given the exposure and any confounders. (iii) Exclusion restriction: the genetic variant only affects the outcome through the exposure. All our exposure and outcome data are selected based on this criterion. The population selected for this study consisted of an independent, general European cohort with strong statistical power in disease association and large-scale aggregate data. The ethnic backgrounds among the samples were similar, ensuring that the genetic variations associated with risk factors identified in the first sample were reliable predictors of risk in the outcome dataset and were not influenced by race or other confounders. Mendelian randomization analysis (MVMR) accounts for the relationships between multiple independent and dependent variables to study complex causal networks.

Methods

Study design

This study constitutes a retrospective observational study employing a two-sample MR approach to analyze SNPs and deduce the relationships between the MRI metrics of essential human organs and liver disease. Utilizing data from the GWAS Catalog platform, which offers publicly available human genome information, we identified single nucleotide polymorphisms (SNPs) that hold significant statistical relevance to MRI-based measurements or derived metrics of key human organ indicators and serve as genetic instrumental variables. Subsequently, leveraging the Finnish FINN project's R9 version of the biogenetic resource library, we focused on outcomes such as nonalcoholic fatty liver disease, nonalcoholic cirrhosis, and primary hepatocellular carcinoma. The study pinpointed SNPs associated with both the MRI metrics of vital organs and liver disease outcomes. We used the Steiger directional test and sensitivity results to control reverse causality, eliminate the influence of unmeasured confounding factors, providing a reference for the detection, diagnosis, and prevention of liver diseases at different levels of progression (Fig. 1).

Inclusion, screening, and determination of exposures and outcomes

We sorted various variables related to body composition measurement indicators currently available in public databases, which were mainly instrument-measurable exposure factors (see Table 1 for details). Nonalcoholic fatty liver disease, cirrhosis, and liver cancer were included as disease outcomes. Various types of hepatitis and alcoholic fatty liver were not included this time. This is because the cause of the former comes from various biologically uncontrollable factors, such as viruses [12], making it unsuitable to apply the MR genetic analysis method in this case, and because the cause of the latter

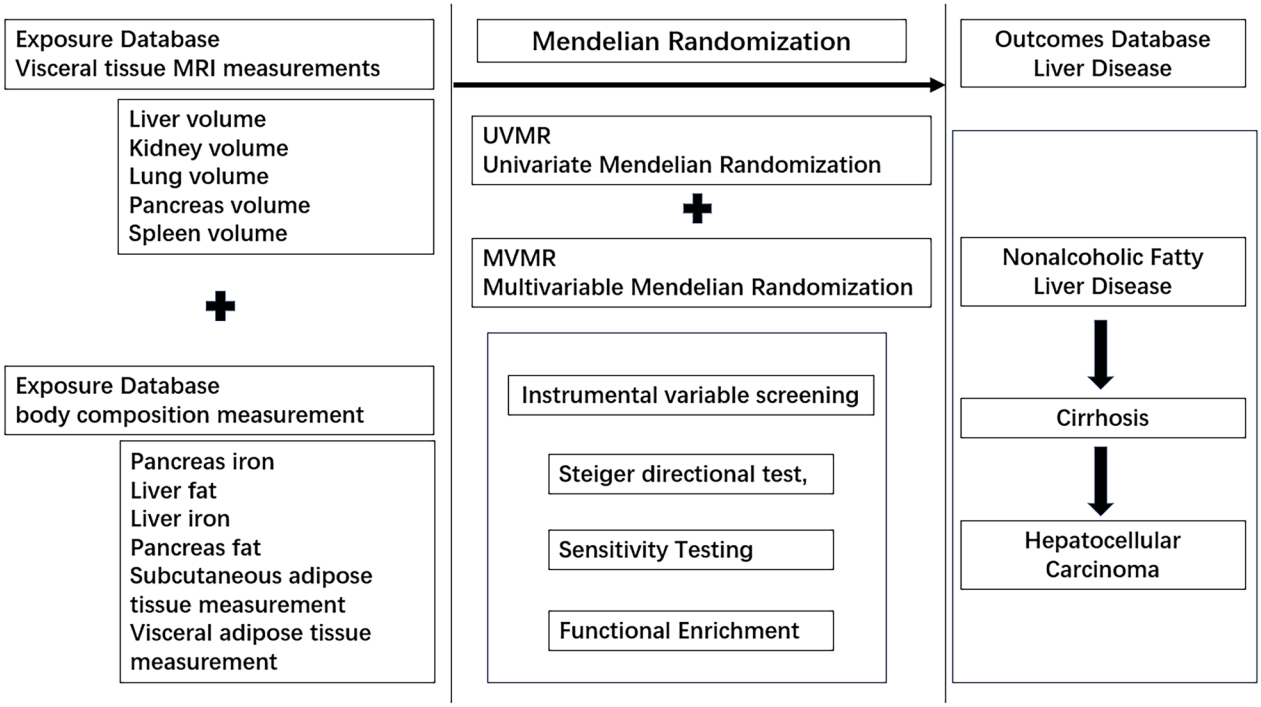

Fig. 1 Schematic diagram of the research design

Table 1 Data summary information of the genome-wide association study database of MRI measurement indicators of major human organs

Exposure/outcome	Abbreviation	Definition	GWASID	Sample size	Year of publication
Liver volume	LV	The MRI protocol (imaging-derived phenotypes, IDPs) of the UKBB	GCST90016666	32,860	2021
Pancreas iron	PI	Same as above	GCST90016676	32,860	2021
Kidney volume	KV	Same as above	GCST90016670	32,860	2021
Liver fat	LF	Same as above	GCST90016673	32,860	2021
Liver iron	LI	Same as above	GCST90016674	32,860	2021
Lung volume	LUV	Same as above	GCST90016668	32,860	2021
Pancreas fat	PF	Same as above	GCST90016675	32,860	2021
Pancreas volume	PV	Same as above	GCST90016669	32,860	2021
Spleen volume	SV	Same as above	GCST90016667	32,860	2021
Subcutaneous adipose tissue measurement	SATM	Same as above	GCST90016672	32,860	2021
Visceral adipose tissue measurement	VATM	Same as above	GCST90016671	32,860	2021
Nonalcoholic fatty liver disease	NAFLD	ICD10	finngen_R9_NAFLD	375,000	2023
Cirrhosis of the liver	NAC	ICD10	finngen_R9_CHIRHEP_NAS	373,300	2023
Hepatocellular carcinoma	HCC	ICD10	finngen_R9_C3_HEPATOCELLU	287,137	2023

is very clear, giving it no research value. To organize the biological database included in the analysis, the variables were initially arranged according to the position order and correlation of human body parts, and then the instrumental variables were extracted.

Data source

MRI metrics of vital human organs, derived from data published by the UK Biobank and integrated into the GWAS Catalog platform, encompass measurements of organ composition and volume, including the

liver, spleen, lung, and pancreas. The aggregate dataset included 32,860 European subjects. We conducted a pooled analysis of 11 MRI assessments of fat and muscle tissue distribution among Caucasian participants from the UK Biobank (average age 64.5 years; 51.4% female). Ultimately, 11 MRI metrics were selected for the exposure group.

For the disease outcome group, we utilized data from the FinnGen project's R9 version of the biogenetic resource database, focusing on liver disease outcomes. The specific conditions analyzed were nonalcoholic fatty liver disease (375,000 cases), nonalcoholic cirrhosis (373,300 cases), and primary hepatocellular carcinoma (287,137 cases). The disease categorization adheres strictly to the International Classification of Diseases, Tenth Revision (ICD- 10).

In our study, we cataloged as exposure factors the MRI measurement variables of major human organs from public databases, as outlined in Table 1.This study utilizes publicly accessible aggregate data and consequently does not necessitate approval from an ethics committee. Furthermore, it adheres to the guidelines of Strengthening the Reporting of Observational Studies in Epidemiology Using Mendelian Randomization (STROBE-MR) [13, 14].

Instrumental variable selection

In MR studies, single nucleotide polymorphisms (SNPs) from the exposure dataset serve as instrumental variables (IVs). These IVs must satisfy three fundamental criteria: (1) a strong association with the exposure; (2) no association with potential confounding factors; and (3) an influence on disease outcomes solely through their relationship with the exposure. SNPs chosen from publicly available GWAS summary data should display genome-wide significance ($P < 5 \times 10^{-8}$) and have a minor allele frequency greater than 0.01.

Instrumental variable screening entails the following procedures: (1) identifying SNP sites that exhibit genome-wide significance ($P < 5 \times 10^{-8}$) correlated with MRI measurement indicators of human internal organs. (2) To mitigate the effects of SNP linkage disequilibrium on the analysis, the linkage disequilibrium parameter, r2, is set below 0.01. Additionally, to ensure the independence of these variants from the GWAS, SNPs are spaced no closer than 10,000 kb apart. This spacing helps eliminate potential biases due to gene pleiotropy. (3) Extract SNP information related to screen exposure from the liver disease database. In instances where the outcome data lack exposure-related SNPs, identify and choose suitable proxy SNPs with an r^2 greater than 0.8. (4) SNPs associated not only the three liver diseases, but also through other pleiotropy phenotypes were removed, and palindromic alleles with incompatible alleles or intermediate allele frequencies were excluded.

Mendelian randomization analysis

This study employs the univariable and multivariable methods of two-sample MR to identify statistically significant features through single-factor analysis and incorporates these features in a multifactorial MR to further refine the selection of instrumental variables. This process also adjusts for and removes confounding and pleiotropic effects among variables, thereby approximating the statistical results more closely to the objective causal effects.

In the two-sample MR analysis, we explored the causal links between the radiological measurement indices of various human organs and liver disease outcomes using five MR methods: inverse-variance weighted analysis (IVW), weighted median, simple mode, weighted mode, and MR-Egger regression. IVW was chosen as the primary method of analysis, with weighted median, simple mode, weighted mode, and MR-Egger regression as supplementary references.

Steiger directional test, sensitivity testing and functional enrichment

We conducted sensitivity analyses using heterogeneity and pleiotropy tests, followed by the MR pleiotropy residual sum and outlier (PRESSO) test to detect and calibrate outliers influenced by horizontal pleiotropy. *Steiger directional test showed the direction of causal relationship is reliable* (Supplement Table 1). We employed an outlier-corrected method within the model to eliminate outliers among the instrumental variables and conducted a second assessment of the effects after correcting for horizontal pleiotropy to ensure the reliability of the MR evaluation. The IVs selected through these steps were used as instrumental variables in the MR analysis. We annotated the genes and performed functional enrichment analysis using the MAGMA analysis method.

Statistical analysis

Statistical analysis was conducted using the two-sample MR (version 0.5.6) and MR-PRESSO (version 1.0) packages for R software (version 4.1.1). Causal effects were quantified using odds ratios (ORs). Unless otherwise specified, the level of statistical significance was set at a two-sided $\alpha = 0.05$.

Results

Instrumental variables

According to the instrumental variable screening criteria of this study, 86 SNPs related to MRI detection indicators of human major internal organs and liver disease

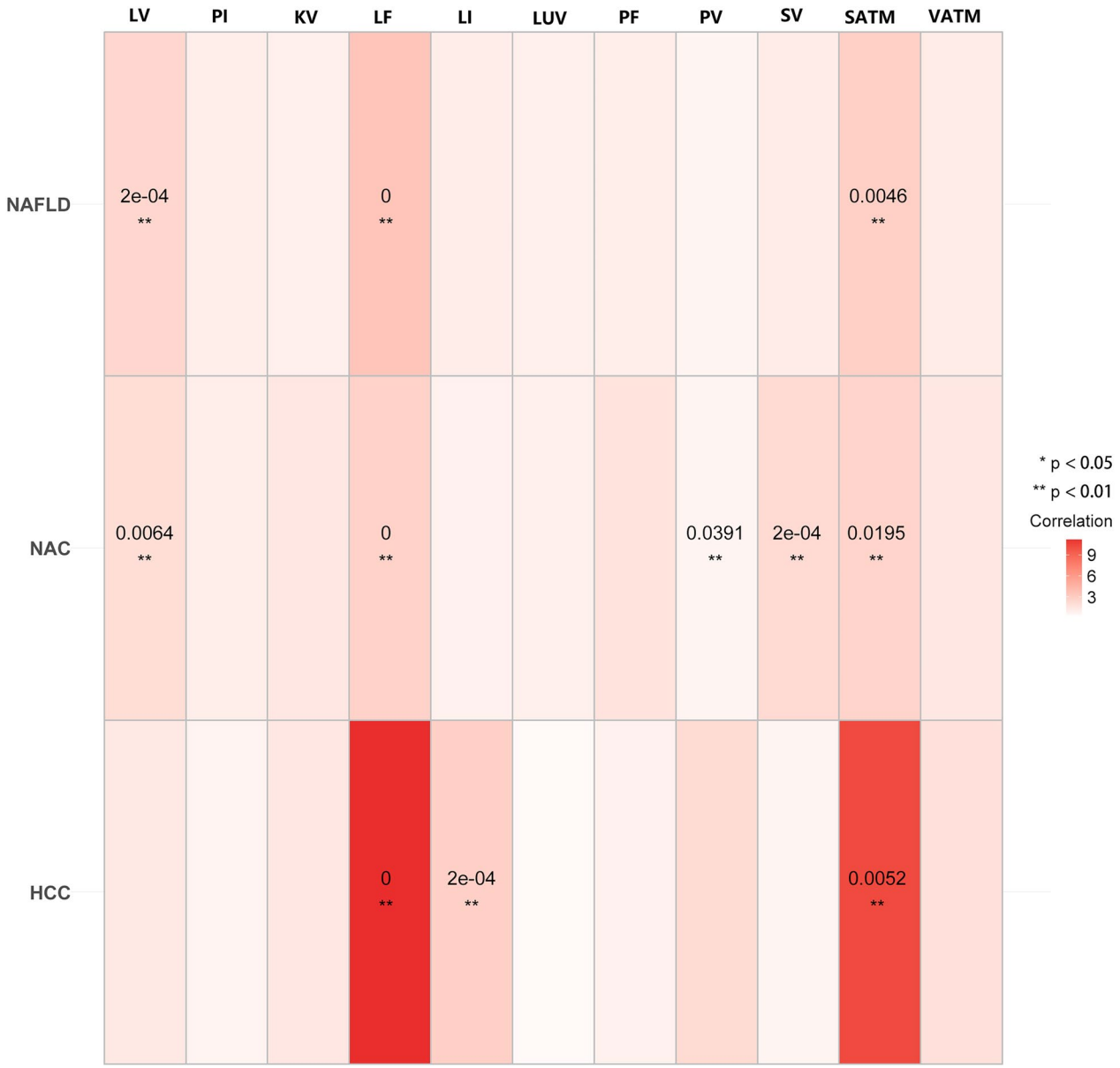

Fig. 2 The correlation between different exposures and outcomes

outcomes (outcomes in this study include nonalcoholic fatty liver disease, cirrhosis and hepatocellular liver cancer) were screened. Supplement Table 1 shows the basic characteristics of these SNPs. Supplementary Fig. 1 shows the SNP density plot and Manhattan plot of disease exposure factors.

Figure 2 illustrates the causal correlation between GWAS exposure variables and various liver disease outcomes. The heatmap analysis highlights that three MRI measurement indicators—liver volume (LV), liver fat (LF), and subcutaneous adipose tissue mass (SATM)—are significantly associated with nonalcoholic fatty liver disease, each showing P values below 0.01. For liver cirrhosis, LV, LF, and SATM also demonstrate significant correlations, with particularly strong associations noted between LV, LF and liver cirrhosis, each with P values below 0.01, while the correlation between SATM and liver cirrhosis shows a P value below 0.05. Furthermore, the analysis identified significant correlations between portal vein (PV) size and spleen volume (SV) with liver cirrhosis outcomes, registering *P* values below 0.05 and 0.01, respectively. Additionally, the correlations between LV, liver iron (LI), and SATM with the outcome of

hepatocellular carcinoma are also statistically significant, with all P values less than 0.01.

Univariate Mendelian randomization analysis

The univariate Mendelian randomization (UVMR) analysis identifies liver volume (LV), liver fat (LF), and subcutaneous adipose tissue mass (SATM) as significant risk factors for nonalcoholic fatty liver disease, with the following odds ratios (ORs) and 95% confidence intervals (CIs): LV: OR = 2.42, 95%CI: 1.52–3.84; LF: OR = 3.52, 95%CI: 2.79–4.43; SATM: OR = 2.87, 95%CI: 1.38–5.94. For liver cirrhosis, the analysis similarly underscores LV, LF, and SATM as risk factors, demonstrating significant associations: LV: OR = 2.04, 95%CI: 1.22–3.41; LF: OR = 2.75, 95%CI: 1.98–3.83; SATM: OR = 2.64, 95%CI: 1.17–5.97. In contrast, the UVMR results indicate a unique correlation between pancreatic volume (PV) and spleen volume (SV) with liver cirrhosis outcomes, suggesting that PV acts as a protective factor (OR = 0.64, 95%CI: 0.42–0.98) while SV is a causative factor (OR = 2.23, 95%CI: 1.46–3.41). In hepatocellular carcinoma (HCC), the results reveal LF, liver iron (LI), and SATM as substantial risk factors, with notably high ORs: LF: OR = 11.42, 95%CI: 5.65–23.10; LI: OR = 2.86, 95%CI: 1.65–4.96; SATM: OR = 10.36, 95%CI: 2.01–53.45 (Fig. 3).

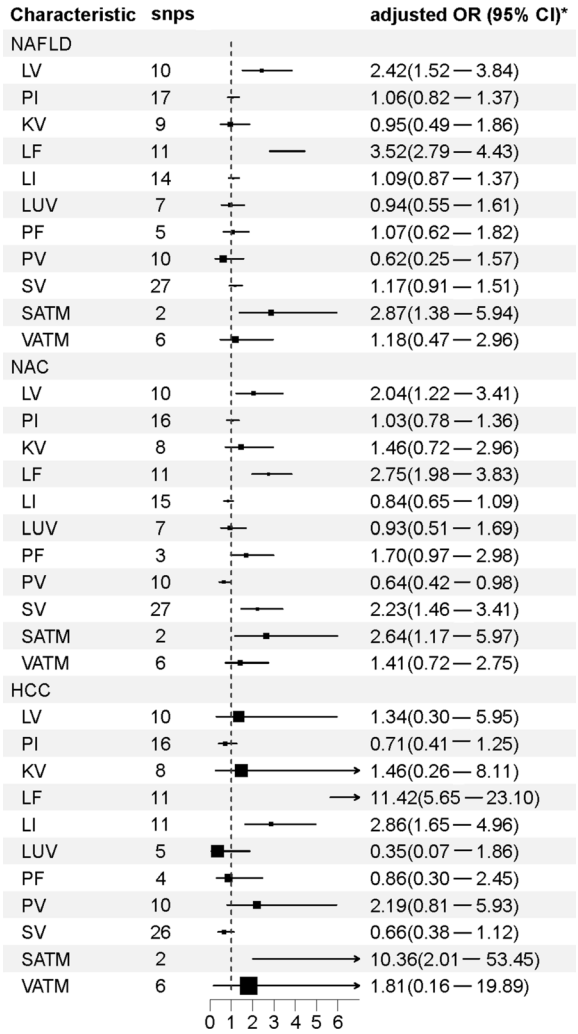

Fig. 3 Univariate Mendelian random analysis results

Multivariate Mendelian randomization analysis

The UVMR results indicate that liver volume (LV), liver fat (LF), and subcutaneous adipose tissue measurement (SATM) are risk factors for NAFLD, with statistically significant findings (LV: OR = 2.42, 95% CI: 1.52–3.84; LF: OR = 3.52, 95% CI: 2.79–4.43; SATM: OR = 2.87, 95% CI: 1.38–5.94). The MVMR results for NAFLD show that LV and LF continue to have statistically significant differences, while SATM no longer supports this (LV: OR = 2.19, 95% CI: 1.48–3.24; LF: OR = 2.75, 95% CI: 2.21–3.44; SATM: OR = 0.91, 95% CI: 0.52–1.60). Similarly, the UVMR results for NAC suggest that LV, LF, and SATM are risk factors for NAC, with significant differences (LV: OR = 2.04, 95% CI: 1.22–3.41; LF: OR = 2.75, 95% CI: 1.98–3.83; SATM: OR = 2.64, 95% CI: 1.17–5.97). The MVMR results for NAC continue to indicate that LV and LF are strong pathogenic factors for cirrhosis, similar to the situation in NAFLD, and that SATM no longer supports significant differences (LV: OR = 6.24, 95% CI: 1.22–31.92; LF: OR = 1.87, 95% CI: 1.00–3.48; SATM: OR = 0.88, 95% CI: 0.31–2.47). Unlike NAFLD, the UVMR results for NAC suggest a strong association between pancreatic volume (PV), splenic volume (SV), and disease endpoints, indicating that PV is a protective factor and SV is a pathogenic factor for NAC (PV: OR = 0.64, 95% CI: 0.42–0.98; SV: OR = 2.23, 95% CI: 1.46–3.41). The MVMR results for NAC similarly indicate that both factors remain significant (PV: OR = 0.16, 95% CI: 0.09–0.28; SV: OR = 0.63, 95% CI: 0.41–0.97). For hepatocellular carcinoma (HCC), both UVMR and MVMR analyses suggest that LF and liver iron (LI) are risk factors. The UVMR results for HCC show that LF, LI, and SATM are risk factors for HCC (LF: OR = 11.42, 95% CI: 5.65–23.10; LI: OR = 2.86, 95% CI: 1.65–4.96; SATM: OR = 10.36, 95% CI: 2.01–53.45). The MVMR results for HCC indicate that LF and LI are risk factors, while SATM no longer supports this (LF: OR = 3.92, 95% CI: 3.00–5.10; LI: OR = 1.03, 95% CI: 0.79–1.34; SATM: OR = 0.95, 95% CI: 0.43–2.09) (Fig. 4; Table 2).

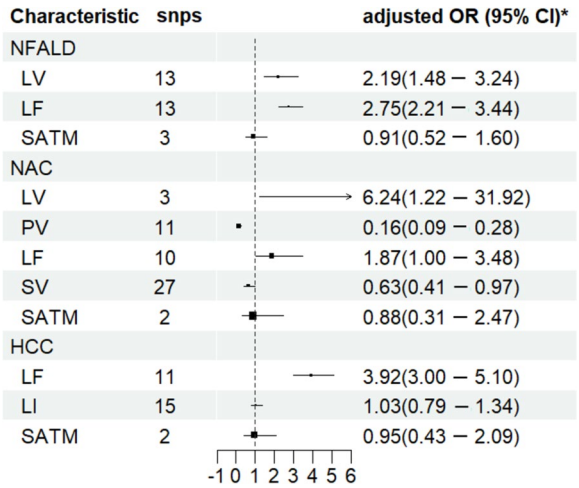

Fig. 4 Multivariate Mendelian random analysis results

Sensitivity testing and functional enrichment

F-value screening instrumental variables

For instrumental variables, we calculated the F-values of all IVs. All these F-values were above 10, which is a level with a strong correlation with disease exposure outcomes and can effectively avoid the weak correlation bias of influencing factors. Due to the excessive number and length of IVs, it is impossible to display them one by one in the main text, so we have included the specific results in the supplementary materials of the article.

FDR correction for statistical thresholds

Bonferroni correction is the most stringent method [15]. This conservative Bonferroni method often ignores potential significance, so we used the milder FDR correction method, which is a multiple comparison correction approach proposed by Benjamini and Hochberg (BH) in 1995. There are many algorithms among which the BH method is widely used.

Variables with statistical significance in the USMR and the three disease endpoints were included in the BH adjustment. The comparisons of the p-value results before and after are shown in Table 3. It can be seen that after adjustment, except for the statistical association between PV and NAC, which is no longer statistically significant, the remaining variables that were previously significant are still supported. Subsequent MVMR analysis will not be corrected because its data usage process is different from that of UVMR and variables are included at the same time.

Sensitivity test

Sensitivity testing of the data suggested that LF was heterogeneous and that SV and VATM may have a certain degree of pleiotropic effects. However, after we used the MR-PRESSO method to remove outliers from the data, indicating heterogeneity in Table 4, the univariate MR results were still significant, indicating that the heterogeneity in the data did not change the results.

In the supplementary material, we also plotted the statistical effect of each SNP, plotted SNP-related leave-one plots and scatter plots, and used the leave-one-out plot method to test whether there were outliers in the SNPs. We observed the symmetry of the funnel plot to check whether the results were stable and evaluated the impact of outliers on the results. After excluding a single SNP each time using the leave-one-out method, the IVW

Table 2 Results of multivariate Mendelian randomization analysis

Characteristic	nsnp	b	se	pval	or	or_lci95	or_uci95
NAFLD							
LV	13	0.783142	0.200632	9.49E− 05	2.188337	1.476839	3.242615
LF	13	1.01276	0.113243	3.78E− 19	2.753189	2.205169	3.437402
SATM	3	− 0.09316	0.286994	0.745491	0.911052	0.519097	1.598959
NAC							
LV	3	1.831754	0.832343	0.027756	6.244828	1.221845	31.91719
PV	11	− 1.84277	0.284333	9.11E− 11	0.158378	0.090712	0.276518
LF	10	0.625295	0.316764	0.048381	1.868797	1.004448	3.476937
SV	27	− 0.45511	0.218329	0.037113	0.634378	0.413526	0.97318
SATM	2	− 0.13003	0.527745	0.805379	0.878067	0.312106	2.470319
HCC							
LF	11	1.364894	0.135062	5.21E− 24	3.915308	3.004684	5.101914
LI	15	0.027211	0.134351	0.839499	1.027584	0.789689	1.337146
SATM	2	− 0.05466	0.403889	0.892357	0.946812	0.429009	2.089589

Table 3 FDR correction results

P-value	LV	LF	LI	PV	SV	SATM
Raw.p						
NFALD	0.000177	1.56E− 26	0.453741	0.343617	0.208621	0.004624
NAC	0.006408	1.87E− 09	0.19134	0.039111	0.000224	0.019489
HCC	0.698477	1.24E− 11	0.000191	0.122895	0.121297	0.005245
Adjust.p						
NFALD	0.00053	4.68E− 26	0.453741	0.343617	0.208621	0.007868
NAC	0.009612	1.87E− 09	0.28701	0.117334	0.000671	0.019489
HCC	0.698477	1.86E− 11	0.000572	0.184343	0.181945	0.007868

Table 4 Sensitivity test results

Test	LV	PI	KV	LF	LI	LUV	PF	PV	SV	SATM	VATM
Heterogeneity_test Q_pval											
NFALD	0.1408	0.0594	0.1949	2.390e− 05	0.2086	0.7814	0.1678	0.1769	0.5810	0.5810	0.0514
NAC	0.0692	0.7126	0.0999	0.0182	0.1498	0.7546	0.3725	0.7237	0.0241	0.7784	0.4538
HCC	0.0586	0.9506	0.0294	0.0006	0.9247	0.9341	0.4083	0.1837	0.4318	0.4362	0.6682
Pleiotropy_test egger_intercept pval											
NFALD	0.8535	0.6060	0.8890	0.8535	0.2086	0.1089	0.5754	0.4696	0.1769	0.3045	0.3133
NAC	0.3005	0.6632	0.8739	0.8390	0.4092	0.8367	0.7148	0.9724	0.0177	0.5638	0.1735
HCC	0.5088	0.9349	0.7945	0.7469	0.7856	0.7774	0.9557	0.9869	0.1268	0.6060	0.0202

method was used to calculate the statistical effects of all remaining SNPs to determine the impact of a single SNP on the estimated value of causal judgment.

Functional enrichment

The significant functional pathways are (Supplementary Table 2):

CHIARADONNA_NEOPLASTIC_TRANSFORMATION_CDC25_DN;CHIARADONNA_NEOPLASTIC_TRANSFORMATION_KRAS_DN;REACTOME_INTRACELLULAR_SIGNALING_BY_SECOND_MESSENGERS;REACTOME_PTEN_REGULATION;COULOUARN_TEMPORAL_TGFB1_SIGNATURE_DN;CREIGHTON_ENDOCRINE_THERAPY_RESISTANCE_4;ACEVEDO_LIVER_CANCER_UP.

The above pathways are closely related to tumorigenesis, intracellular damage and death, and the development of liver lesions. This shows the reliability of our results to a certain extent.

Discussion

Nonalcoholic fatty liver disease

The UVMR results show that LV, LF, and SATM are all risk factors for NAFLD, and the statistical results show that they are significant. The endpoint of fatty liver disease used this time is nonalcoholic fatty liver, which excludes the confounding effect of alcohol consumption. Liver volume is highly correlated with NAFLD. The reasons for the increase in liver volume are complex. The most important ones are obesity and the accumulation of fat in the abdomen and liver. The long-term development of this condition can easily lead to fatty liver. The above results support the previous common sense in disease diagnosis. LF and SATM are liver fat content and skin tissue fat content. These two factors have the same pathogenic mechanism as LV. The above two variables should be a verification of past common sense and suggest that the results of this analysis are relatively convincing from a certain perspective. However, VATM, or visceral fat content, does not support a relationship with NAFLD, indicating that the distribution location of adipose tissue is key to the onset of NAFLD. Only the long-term accumulation of fat near the liver can easily induce NAFLD. The MVMR results for NAFLD show that LV and LF continue to have significant differences, but SATM no longer supports this. This illustrates the importance of fat accumulation in the human body and further confirms the results of UVMR. The above results have been similarly reported in many articles [16], and this result verifies these previous conclusions [17].

Cirrhosis (NAC)

The UVMR results of NAC also suggest that LV, LF, and SATM are risk factors for liver cirrhosis, with significant differences. This shows that the long-term excessive accumulation of fat is also an important cause of liver cirrhosis [18]. The MVMR results continue to suggest that LV and LF are highly pathogenic to cirrhosis. Similar to the situation in NAFLD, SATM no longer supports significant differences.

Unlike NAFLD, the UVMR results of NAC suggest a high correlation between the two factors of PV and SV and disease endpoints. The results suggest that the former is a protective factor of NAC and that the latter is a causative factor of NAC. The MVMR results also suggest that both are still meaningful. There are few similar reports on this [19]. However, there are many similar reports on the close relationship between the liver and spleen [20]. This report shows that an increase in PV can reduce the occurrence of NAC and is a protective factor. The pancreas is an important endocrine organ in the human body that has exocrine and endocrine functions [21]. The pancreas plays an important role in human energy metabolism and fat tissue metabolism. In particular, the pancreas can secrete lipase, which can break down fat, promote the utilization of fat in the body, and reduce fat accumulation. Congenital dysplasia of the pancreas often means that the pancreas is congenitally small and is more likely to develop pancreatic insufficiency, chronic severe exocrine insufficiency. Once blood sugar levels rise, it is difficult for pancreatic beta cells to secrete enough insulin to lower blood sugar concentrations[22]. Such long-term high-sugar environment stimulation of the body will cause beta cells to become less sensitive to blood sugar changes, resulting in insulin resistance; this in turn leads to abnormal blood sugar conversion, inducing fatty liver, cirrhosis, etc. [23].

The spleen and liver are adjacent. In both Chinese medicine and Western surgery, the liver and spleen are juxtaposed [24–26], indicating that the two are closely related. The spleen is an important immune and lymphatic organ in the human body. Inflammation and disease can induce functional swelling of the spleen. The causes of congenital splenomegaly may include congenital genetic metabolic diseases, autoimmune hemolytic disease and other autoimmune mechanism defects [27]. Autoimmune hepatitis, also known as autoimmune hepatitis, is a complex, chronic, progressive inflammatory disease caused by the body's immune system mistakenly attacking its own liver tissue. It not only has a serious impact on liver function, but may also further develop into cirrhosis[28, 29].

Primary hepatocellular carcinoma (i.e., primary liver cancer, HCC)

Both the UVMR results and MVMR analysis of HCC show completely different situations from NAFLD and NAC. It is suggested that LF and LI are risk factors for HCC, while LV no longer shows statistical significance. Although liver fat is suggested to be the cause of HCC, the cause may be quite different from NAFLD and NAC. Only when the accumulation of adipose tissue causes steatohepatitis or liver cell swelling, destroys the normal liver lobule structure, and causes liver function damage will HCC occur.

What deserves attention is the high pathogenicity of LI to HCC. Most previous studies have suggested that excessive liver iron content may be related to liver function damage, In this study, it shows a strong direct correlation with HCC, indicating that excessive liver iron load may predispose to liver cancer. Free ferrous ions are mainly deposited in hepatic parenchymal cells, increasing the production of lipid peroxidation products through the Fenton reaction and inducing cell damage, combine with reactive oxygen species to catalyze the production of free radicals, damaging DNA, proteins, and lipids, leading to severe liver cell and tissue damage leading to liver fibrosis[30]. NAFLD can inhibit hepatic hepcidin and upregulate DMT1 (divalent metal transporter 1, DMT1) by inducing oxidative stress, exacerbating liver iron accumulation and promoting liver damage. It can also induce hepatocyte ferroptosis by activating iron metabolism-related genes (such as FTH1, TFR1, GPX4), promoting the development of HCV infection into hepatocellular carcinoma [31]. In many patients with iron overloading the expression of hepcidin were reduced [32], and the reduction in hepcidin levels intensifies this vicious cycle. Excess liver iron also forms iron-containing bodies, which directly damage the structure of liver cells and worsen liver function. The presence of siderosomes can also trigger an immune response, produce inflammatory factors, and aggravate liver cell damage. The occurrence of the above mechanisms may be the cause of LI's pathogenesis of HCC.

Although the analysis results this time only suggested the disease-promoting effect of liver iron content on liver cancer, some studies have shown that similar effects are manifested to varying degrees in the process of MASLD and liver cirrhosis. Recent studies have shown, hepatic iron accumulation can activate ferroptosis by upregulating the c-Myc-ACSL4 vector, thereby promoting the development of MASH [33]. The results of some MAFLD clinical specimens and experimental model studies have shown that compared with the normal group or normal fatty liver group, the serum ferritin level in the MASH group was significantly increased, and the serum ferritin

level was significantly correlated with hepatic cell iron accumulation [34, 35], suggesting that serum ferritin levels in MAFLD are related to ferroptosis.

Functional enrichment

CHIARADONNA_NEOPLASTIC_TRANSFORMATION_CDC25_DN and CHIARADONNA_NEOPLASTIC_TRANSFORMATION_KRAS_DN, these two pathways described the genes down-regulated in NIH3 T3 cells (fibroblasts) transformed by activated KRAS (GeneID3845) vs those reverted to normal cells upon over-expression of a dominant negative form of CDC25 (GeneID5923) [36]. This pathway linked our enrichment results directly to gene activation the alteration in energy metabolism of cancer cells, their fragility towards glucose shortage and ensuing apoptotic death. ACEVEDO_LIVER_CANCER_UP pathway described genes up-regulated in hepatocellular carcinoma (HCC) compared to normal liver samples[37]. This result links the instrumental variables of this study with the gene expression characteristics of human liver tumor pathogenesis, suggesting the reliability of our results.

At the same time, based on the MR analysis results of NAFLD, NAC, and HCC, combined with the timeliness of the occurrence of the three diseases, the occurrence mechanisms of the first two are relatively close because the influencing factors are also relatively similar. The mechanism of HCC is quite different from the first two, and a considerable part of HCC is caused by liver function damage factors. In addition, PV and SV play only a significant role when the disease progresses to the NAC stage but are not significant in the NAFLD stage. Currently, no definitive clinical evidence exists to establish a correlation between MRI indicators for various human organs and liver lesions. This shows that all the influencing factors observed in this study have an impact on the intervention and progression of the entire pathological trilogy of liver lesions. There is an obvious progressive effect.

Conclusions

This study used two-sample Mendelian randomization analysis to determine the causal relationship between MRI measurement indicators of the main internal organs of the human body and three liver diseases, eliminating the interference of confounding factors and conducting reverse causality analysis. This study shows that LV, LF, and SATM are related to NAFLD, and the NAC stage shows additional pathogenic effects of PV and SV. The results related to LI support the pathogenic effect of liver iron factors in the HCC stage.

Abbreviations

MR	Mendelian randomization
SNPs	Single nucleotide polymorphisms
IVW	Inverse-variance weighted analysis
ORs	Odds ratios
CIs	Confidence intervals
UVMR	Univariate Mendelian randomization analysis
LV	Liver volume
LF	Liver fat
SATM	Subcutaneous adipose tissue measurement
NAFLD	Nonalcoholic fatty liver disease
PV	Pancreatic volume
SV	Splenic volume
HCC	Hepatocellular carcinoma
LI	Liver iron
SFL	Simple fatty liver
MRI	Magnetic resonance imaging
MAFLD	Metabolic fatty liver disease
BMI	Body mass index
GWAS	Genome-wide association studies

Supplementary Information

The online version contains supplementary material available at https://doi.org/10.1186/s40001-025-02529-z.

Supplementary Fig. 1 SNP density map and Manhattan plot of disease exposure factors

Supplementary Table 1 Basic characteristics of SNP

Supplementary Table 2 Functional enrichment results

Acknowledgements

We would like to acknowledge the creators and maintainers of the public GWAS database, which was instrumental in our analyses. Their efforts to maintain high-quality, accessible data are deeply appreciated.

Author contributions

WHY: Protocol design, data analysis, and manuscript writing and editing. ZDJ: Contributing to manuscript writing and editing. ZJG: Literature review, data analysis. TJC: Literature review, bioinformation analysis. GJ: Literature review, project planning and revision, oversight of experimental projects, and manuscript review and enhancement.

Funding

N/A.

Availability of data and materials

The data produced and examined in this study can be obtained from the corresponding author when a justifiable request is made. Furthermore, the materials employed in this investigation can also be accessed for non-commercial usage, upon request. Inquiries concerning access to data or materials should be addressed to the corresponding author.

Declarations

Ethics approval and consent to participate

N/A.

Consent for publication

N/A.

Competing interests

The authors declare no competing interests.

Received: 16 July 2024 Accepted: 28 March 2025
Published online: 11 April 2025

References

1. Li D, Zhang M, Wu S, Tan H, Li N. Risk factors and prediction model for nonalcoholic fatty liver disease in northwest China. Sci Rep. 2022;12(1):13877.
2. Byrne CD, Targher G. NAFLD: a multisystem disease. J Hepatol. 2015;62(1 Suppl):S47-64.
3. Xia T, Du M, Li H, Wang Y, Zha J, Wu T, Ju S. Association between liver MRI proton density fat fraction and liver disease risk. Radiology. 2023;309(1): e231007.
4. Chiheb S, Cosson E, Banu I, Hamo-Tchatchouang E, Cussac-Pillegand C, Nguyen MT, Valensi P. Are obese individuals with no feature of metabolic syndrome but increased waist circumference really healthy? A cross sectional study. Exp Clin Endocrinol Diabetes. 2016;124(7):410–6.
5. Samuel VT, Shulman GI. Nonalcoholic fatty liver disease as a nexus of metabolic and hepatic diseases. Cell Metab. 2018;27(1):22–41.
6. Sim BC, Kang YE, You SK, Lee SE, Nga HT, Lee HY, Nguyen TL, Moon JS, Tian J, Jang HJ, et al. Hepatic T-cell senescence and exhaustion are implicated in the progression of fatty liver disease in patients with type 2 diabetes and mouse model with nonalcoholic steatohepatitis. Cell Death Dis. 2023;14(9):618.
7. Lemos T, Gallagher D. Current body composition measurement techniques. Curr Opin Endocrinol Diabetes Obes. 2017;24(5):310–4.
8. Metoyer CJ, Sullivan K, Winchester LJ, Richardson MT, Esco MR, Fedewa MV. Body composition estimates using a 2D image analysis system across different environmental conditions: an agreement study. J Biophotonics. 2024;17(4): e202300518.
9. Salmon-Gomez L, Catalan V, Fruhbeck G, Gomez-Ambrosi J. Relevance of body composition in phenotyping the obesities. Rev Endocr Metab Disord. 2023;24(5):809–23.
10. Landau D, Stout J, Presley LH, O'Tierney-Ginn P, Groh-Wargo S, Catalano PM. Reliability of routine anthropometric measurements to estimate body composition in term infants. Pediatr Res. 2021;89(7):1751–5.
11. Liu J, Zhou H, Zhang Y, Huang Y, Fang W, Yang Y, Hong S, Chen G, Zhao S, Chen X, et al. Docosapentaenoic acid and lung cancer risk: a Mendelian randomization study. Cancer Med. 2019;8(4):1817–25.
12. Zhang H, Gao S, Pei R, Chen X, Li C. Hepatitis C virus-induced prion protein expression facilitates hepatitis C virus replication. Virol Sin. 2017;32(6):503–10.
13. Skrivankova VW, Richmond RC, Woolf BAR, Davies NM, Swanson SA, VanderWeele TJ, Timpson NJ, Higgins JPT, Dimou N, Langenberg C, et al. Strengthening the reporting of observational studies in epidemiology using mendelian randomisation (STROBE-MR): explanation and elaboration. BMJ. 2021;375: n2233.
14. Skrivankova VW, Richmond RC, Woolf BAR, Yarmolinsky J, Davies NM, Swanson SA, VanderWeele TJ, Higgins JPT, Timpson NJ, Dimou N, et al. Strengthening the reporting of observational studies in epidemiology using Mendelian randomization: the STROBE-MR statement. JAMA. 2021;326(16):1614–21.
15. Ye Z, Wang Z, Hou Y. Does Bonferroni correction "rescue" the deviation from Hardy-Weinberg equilibrium? Forensic Sci Int Genet. 2020;46: 102254.
16. Valenzuela-Vallejo L, Sanoudou D, Mantzoros CS. Precision medicine in fatty liver disease/non-alcoholic fatty liver disease. J Pers Med. 2023;13(5):830.
17. Dong Y, Li G. Cardiac abnormalities in patients with nonalcoholic fatty liver disease: insights from auxiliary examinations. Herz. 2021;46(2):158–63.
18. Zhuang YP, Wang SQ, Pan ZY, Zhong HJ, He XX. Differences in complications between hepatitis B-related cirrhosis and alcohol-related cirrhosis. Open Med (Wars). 2022;17(1):46–52.
19. Ko J, Sequeira IR, Skudder-Hill L, Cho J, Poppitt SD, Petrov MS. Metabolic traits affecting the relationship between liver fat and intrapancreatic fat: a mediation analysis. Diabetologia. 2023;66(1):190–200.
20. Kato H, Hamada T, Kuriyama N, Ito T, Magawa S, Azumi Y, Kishiwada M, Mizuno S, Usui M, Sakurai H, et al. Role of spleen in hepatic ischemia reperfusion injury: splenic congestion during ischemia accelerates leukocyte infiltration within the liver after reperfusion. Hepatol Res. 2017;47(3):E132–41.
21. Martin S, Sorokin EP, Thomas EL, Sattar N, Cule M, Bell JD, Yaghootkar H. Estimating the effect of liver and pancreas volume and fat content on risk of diabetes: a Mendelian randomization study. Diabetes Care. 2022;45(2):460–8.
22. Suenaga M, Yu J, Shindo K, Tamura K, Almario JA, Zaykoski C, Witmer PD, Fesharakizadeh S, Borges M, Lennon AM, Shin EJ, Canto MI, Goggins M. Pancreatic juice mutation concentrations can help predict the grade of dysplasia in patients undergoing pancreatic surveillance. Clin Cancer Res. 2018;24(12):2963–74. https://doi.org/10.1158/1078-0432.CCR-17-2463.
23. Kobayashi T, Aida K, Fukui T, Jimbo E, Shimada A, Mori Y, Fujii T, Yagihashi S. Pancreatic ductal hyperplasia/dysplasia with obstructive chronic pancreatitis: an association with reduced pancreatic weight in type 1 diabetes. Diabetologia. 2016;59(4):865–7. https://doi.org/10.1007/s00125-016-3867-x.
24. Elchaninov A, Vishnyakova P, Sukhikh G, Fatkhudinov T. Spleen: reparative regeneration and influence on liver. Life (Basel). 2022;12(5):626.
25. Heringa MB, Peters RJB, Bleys R, van der Lee MK, Tromp PC, van Kesteren PCE, van Eijkeren JCH, Undas AK, Oomen AG, Bouwmeester H. Detection of titanium particles in human liver and spleen and possible health implications. Part Fibre Toxicol. 2018;15(1):15.
26. Wang L, Wang C, Wang Z, Gan J, Liu C, Xia S, Niu Y, Chen D, Zhang J, Dong L. Transforming the spleen into a liver-like organ in vivo. Sci Adv. 2020;6(24):eaaz974.
27. Chavula T, To S, Smith J, Pedroza M, Nimri J, Devaraj S, Wenderfer S, Vogel TP, Agarwal SK. CADHERIN-11 regulation of myeloid phagocytes and autoimmune inflammation in murine lupus. J Autoimmun. 2024;145: 103197. https://doi.org/10.1016/j.jaut.2024.103197.
28. Zhu M, Deng G, Tan P, Xing C, Guan C, Jiang C, Zhang Y, Ning B, Li C, Yin B, Chen K, Zhao Y, Wang HY, Levine B, Nie G, Wang RF. Beclin 2 negatively regulates innate immune signaling and tumor development. J Clin Invest. 2020;130(10):5349–69. https://doi.org/10.1172/JCI133283.PMID:32865519;PMCID:PMC7524487.
29. Bae JS, Lee DH, Yoo J, Yi NJ, Lee KW, Suh KS, Kim H, Lee KB. Association between spleen volume and the post-hepatectomy liver failure and overall survival of patients with hepatocellular carcinoma after resection. Eur Radiol. 2021;31(4):2461–71.
30. Miyata T, Nagy LE. Programmed cell death in alcohol-associated liver disease. Clin Mol Hepatol. 2020;26(4):618–25. https://doi.org/10.3350/cmh.2020.0142.
31. Armitage AE, Stacey AR, Giannoulatou E, Marshall E, Sturges P, Chatha K, Smith NM, Huang X, Xu X, Pasricha SR, Li N, Wu H, Webster C, Prentice AM, Pellegrino P, Williams I, Norris PJ, Drakesmith H, Borrow P. Distinct patterns of hepcidin and iron regulation during HIV-1, HBV, and HCV infections. Proc Natl Acad Sci U S A. 2014;111(33):12187–92. https://doi.org/10.1073/pnas.1402351111.
32. Sonnweber T, Nachbaur D, Schroll A, Nairz M, Seifert M, Demetz E, Haschka D, Mitterstiller AM, Kleinsasser A, Burtscher M, et al. Hypoxia induced downregulation of hepcidin is mediated by platelet derived growth factor BB. Gut. 2014;63(12):1951–9.
33. Tao L, Yang X, Ge C, Zhang P, He W, Xu X, Li X, Chen W, Yu Y, Zhang H, Chen SD, Pan XY, Su Y, Xu C, Yu Y, Zheng MH, Min J, Wang F. Integrative clinical and preclinical studies identify FerroTerminator1 as a potent therapeutic drug for MASH. Cell Metab. 2024;36(10):2190-2206.e5. https://doi.org/10.1016/j.cmet.2024.07.013.
34. Zhang J, Wang Y, Fan M, Guan Y, Zhang W, Huang F, Zhang Z, Li X, Yuan B, Liu W, Geng M, Li X, Xu J, Jiang C, Zhao W, Ye F, Zhu W, Meng L, Lu S, Holmdahl R. Reactive oxygen species regulation by NCF1 governs ferroptosis susceptibility of Kupffer cells to MASH. Cell Metab. 2024;36(8):1745-1763.e6. https://doi.org/10.1016/j.cmet.2024.05.008.
35. Corradini E, Buzzetti E, Dongiovanni P, Scarlini S, Caleffi A, Pelusi S, Bernardis I, Ventura P, Rametta R, Tenedini E, Tagliafico E, Fracanzani AL, Fargion S, Pietrangelo A, Valenti LV. Ceruloplasmin gene variants are associated with hyperferritinemia and increased liver iron in patients with NAFLD. J Hepatol. 2021;75(3):506–13. https://doi.org/10.1016/j.jhep.2021.03.014.
36. Chiaradonna F, Sacco E, Manzoni R, Giorgio M, Vanoni M, Alberghina L. Ras-dependent carbon metabolism and transformation in mouse fibroblasts. Oncogene. 2006;25(39):5391–404. https://doi.org/10.1038/sj.onc.1209528.
37. Acevedo LG, Bieda M, Green R, Farnham PJ. Analysis of the mechanisms mediating tumor-specific changes in gene expression in human liver tumors. Cancer Res. 2008;68(8):2641–51. https://doi.org/10.1158/0008-5472.CAN-07-5590.